Diffusion-Limited Current in Organic Metal-Insulator-Metal Diodes

P. de Bruyn,[1,2] A. H. P. van Rest,[1] G. A. H. Wetzelaer,[1,2] D. M. de Leeuw,[1,3] and P. W. M. Blom[1,3]

[1]*Zernike Institute for Advanced Materials, University of Groningen, Nijenborgh 4, 9747 AG Groningen, Netherlands*

[2]*Dutch Polymer Institute, Post Office Box 902, 5600 AX Eindhoven, Netherlands*

[3]*Max Planck Institute for Polymer Research, Ackermannweg 10, 55128 Mainz, Germany*

(Received 6 June 2013; revised manuscript received 15 August 2013; published 29 October 2013)

An analytical expression for the diffusion current in organic metal-insulator-metal diodes is derived. The derivation is based on the classical diffusion theory of Schottky, with adaptations to account for the absence of doping, a built-in voltage due to asymmetric contacts, and band bending at the Ohmic contact. The commonly observed deviation of the ideality factor from unity (~ 1.2) is characteristic of diffusion-limited currents in undoped organic semiconductors. Summing with the classical space-charge limited current provides a full analytic description of the current as a function of voltage, temperature and layer thickness.

DOI: 10.1103/PhysRevLett.111.186801 PACS numbers: 73.40.Rw, 72.80.Le

Conjugated polymers and small molecules, as typically used in organic light-emitting diodes or solar cells are undoped semiconductors. When these semiconductors are sandwiched between two electrodes, a metal-insulator-metal (MIM) diode stack is formed. Many organic diodes consist of an Ohmic injecting contact and a non-Ohmic collection contact. In general, when electrodes with different work functions are used an internal electric field will build up resulting from a built-in voltage V_{bi} across the undoped semiconductor, which equals the difference in work function of the electrodes.

As a reference, we consider the case of a hole-only MIM diode with one Ohmic and one non-Ohmic contact, as shown in Fig. 1(a). The collecting contact at $x = L$, where x denotes the position within the diode and L is the film thickness, is separated from the valence band by a barrier height, φ_b. The injecting contact at $x = 0$ aligns with the valence band. For both contacts the energy barrier to the conduction band is so large that electron injection can be neglected. The built-in voltage V_{bi} is then equal to the barrier height φ_b.

At high positive bias on the Ohmic contact, larger than the built-in voltage, the resulting electric field becomes positive, pointing toward the collecting contact. Holes are injected and the current is dominated by drift. The current becomes limited by the uncompensated charges of the injected holes, leading to a space-charge-limited current (SCLC) that can be analytically described by the Mott-Gurney equation [1] as

$$J = \frac{9}{8}\varepsilon\mu\frac{(V - V_{\mathrm{bi}})^2}{L^3}, \tag{1}$$

with ε the dielectric constant, μ the charge-carrier mobility, and V the applied voltage. A large advantage of such an analytical description is that from experimental data on single-carrier devices the charge carrier mobility can directly be obtained from current density versus voltage (J-V) measurements [2].

As shown in Fig. 1(a), we now apply a small positive bias on the injecting contact. When the bias is smaller than the built-in voltage the electric field is still negative, pointing toward the injecting contact. The drift current due to the injected holes is therefore negative. However, the gradient in the hole density leads to diffusion of holes toward the collecting contact. The net positive current then results from the positive diffusion current that dominates over the negative drift current.

Until now the diffusion-limited current in organic MIM diodes has been analyzed using the classical Shockley diode equation [3], given by

$$J = J_0\left[\exp\left(\frac{qV}{\eta kT}\right) - 1\right], \tag{2}$$

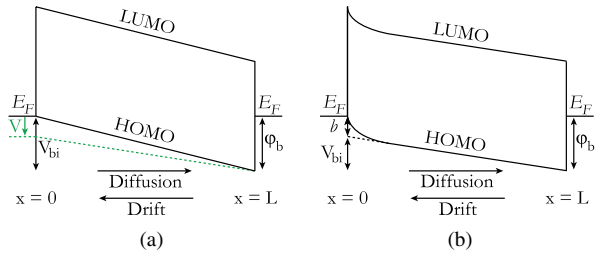

FIG. 1 (color online). Energy-band diagram of an organic hole-only MIM diode, with HOMO and LUMO the highest occupied and lowest unoccupied molecular orbitals, respectively. The layer thickness is L. x denotes the position in the diode. The contact at $x = 0$ is Ohmic, while the collecting contact at $x = L$ is separated from the valence band by a barrier height φ_b. (a) Thermal equilibrium and upon applying a small positive bias smaller than the built-in voltage (dashed line). (b) Band diagram at thermal equilibrium by including band bending due to injected holes at the Ohmic contact.

where J_0 is normally taken as a fit parameter, and η an empirical ideality factor. However, Eq. (2) was derived to describe a bipolar current through a p-n diode, where the ideality factor is strictly related to the order of recombination. Applying this equation to unipolar devices with undoped semiconductors is therefore questionable, but nevertheless frequently used in these cases. It was recently demonstrated that in organic MIM diodes this ideality factor deviates from unity by the presence of energetically deep states within the band gap [4]. However, a remarkable result was that even for organic semiconductors such as poly(9,9-dioctylfluorene) (PFO), the poly(p-phenylene vinylene) (PPV) derivative BEH/BB-PPV, and the fullerene derivative PCBM that all show nondispersive transport, pointing to the absence of deep traps, an ideality factor of typically 1.2 was found instead of unity.

In this Letter, we derive an analytical equation that describes the diffusion current for undoped semiconductors or insulators in MIM diodes with asymmetric contacts. The derivation is based on the classical diffusion model put forth by Schottky [5] for a metal contact on a doped inorganic semiconductor. We show that the derived equation provides a simple and fast method to model diffusion currents in MIM diodes with different contacts. The analytical diffusion model allows for a direct determination of the built-in potential in organic MIM devices, which we verify on hybrid organic light-emitting diodes [6–9] with metal-oxide contacts, which are governed by universal energy alignment [10]. By summing the contributions of drift and diffusion we can now analytically describe the current through the MIM diode in the full voltage range, allowing disentanglement of the drift and diffusion contributions to the current.

The original diffusion theory by Schottky [5] describes the situation for a metal contact on a *doped* semiconductor. In such a Schottky diode, majority carriers diffuse from the semiconductor into the metal to equilibrate the Fermi level. The charge of the remaining uncompensated dopants then leads to the buildup of an electric field in the depletion region, resulting in band bending. A similar model was used by Shockley for the current across a p-n junction, viz. a depletion region formed between a p- and n-doped semiconductor [3]. An alternative theory to describe the current in a Schottky diode, based on thermionic emission, is valid only for high charge-carrier mobilities [11,12], whereas diffusion is the limiting case in low-mobility semiconductors, like organic semiconductors.

In MIM structures, band bending due to uncompensated dopants is absent. Below we will introduce the appropriate boundary conditions [13]. We start with the hole-only MIM diode of Fig. 1(a). Following the classical derivation of Schottky for diffusion currents, the hole current density is given by

$$J_p = \mu_p kT\left(\frac{p}{kT}\frac{dE_v}{dx} - \frac{dp}{dx}\right), \tag{3}$$

where the diffusion coefficient has been replaced by the mobility μ_p through the Einstein relation [4]. However, in contrast to a Schottky diode, the limit for integration in the MIM structure has to be set to the total device thickness L, since the device is fully depleted, leading to

$$J_p \int_0^L \exp\left(-\frac{E_v(x)}{kT}\right)dx = -\mu_p kT p(x)\exp\left(-\frac{E_v(x)}{kT}\right)\Big|_0^L, \tag{4}$$

with p the hole density and E_v the valence-band edge, or, analogously in this case the highest occupied molecular orbital (HOMO) of the polymer. To evaluate this expression we need to introduce the MIM boundary conditions for the charge carrier density $p(x)$ and the valence band $E_v(x)$ at the electrode-semiconductor interfaces $x = 0$ and $x = L$.

As shown in Fig. 1(a) the built-in voltage V_{bi} for this device is equal to φ_b, In that particular case the boundary conditions for the charge-carrier density at the electrodes of a metal-insulator-metal device are given by [13]

$$p(0) = N_v, \tag{5a}$$

$$p(L) = N_v \exp\left(-\frac{q\varphi_b}{kT}\right), \tag{5b}$$

whereas the boundary conditions for the valence band, with respect to the Fermi level of the hole-extraction contact, for $V < V_{\mathrm{bi}}$ are given by

$$E_v(0) = -qV, \tag{6a}$$

$$E_v(L) = -q\varphi_b. \tag{6b}$$

Note that in this case a positive forward bias V at $x = 0$ lowers the internal voltage to φ_b-V, leading to a reduction of the negative drift current of holes toward the injecting contact at $x = 0$, which results in an enhanced positive current in the x direction. Combination with Eq. (4) gives for the current

$$J_p = N_v \mu_p kT\left[\exp\left(\frac{qV}{kT}\right) - 1\right] \Big/ \int_0^L \exp\left(-\frac{E_v(x)}{kT}\right)dx. \tag{7}$$

Because of the absence of space charge there is no band bending in the MIM structure, so the positional dependence of the valence band $E_v(x)$ is just a simple triangular shape, given by

$$E_v(x) = -q\left(V + \frac{(\varphi_b - V)x}{L}\right), \tag{8}$$

yielding

$$\int_0^L \exp\left(-\frac{E_v(x)}{kT}\right)dx = \frac{LkT}{q(\varphi_b - V)}\left[\exp\left(\frac{q\varphi_b}{kT}\right) - \exp\left(\frac{qV}{kT}\right)\right]. \tag{9}$$

Substituting Eq. (9) into Eq. (7) then leads to an analytical current density expression for the diffusion-limited current in a MIM diode, given by

$$J_p = \frac{q\mu_p N_v(\varphi_b - V)\left[\exp\left(\frac{qV}{kT}\right) - 1\right]}{L\left[\exp\left(\frac{q\varphi_b}{kT}\right) - \exp\left(\frac{qV}{kT}\right)\right]}. \quad (10)$$

A similar expression was obtained by Paasch *et al.* [14]. We note that the use of a constant mobility in our derivation is valid since in the diffusion regime the carrier densities in the diode are sufficiently low such that mobility enhancement due to density of states filling [15] does not play a role [16]. Before comparing Eq. (10) to experimental data it is essential to consider that for Ohmic contacts on insulators or undoped semiconductors charge carriers diffuse from the electrode into the semiconductor, forming an accumulation region close to the contact [17]. As shown in Fig. 1(b) the accumulated charge carriers close to the injecting contact at $x = 0$ cause band bending and reduce the built-in voltage of the device. Reported values for this band bending, here described by the parameter b, typically lie in the range of 0.2–0.3 V and depend also on energetic disorder [18–22]. To account for this accumulation we approximate the energy band diagram of the MIM diode by the dashed line in Fig. 1(b). In this way the reduction of the built-in voltage is taken into account, while maintaining the triangular potential. Then the boundary conditions are modified to

$$p(0) = N_v \exp\left(-\frac{qb}{kT}\right), \quad (11a)$$

$$p(L) = N_v \exp\left(-\frac{q\varphi_b}{kT}\right), \quad (11b)$$

$$E_v(0) = -q(V + b), \quad (11c)$$

$$E_v(L) = -q\varphi_b. \quad (11d)$$

The current equation, Eq. (10), is for this case modified to

$$J_p = \frac{q\mu_p N_v(\varphi_b - b - V)\left[\exp\left(\frac{qV}{kT}\right) - 1\right]}{L\exp\left(\frac{qb}{kT}\right)\left[\exp\left(\frac{q(\varphi_b - b)}{kT}\right) - \exp\left(\frac{qV}{kT}\right)\right]}. \quad (12)$$

Clearly, the band-bending parameter b does not only reduce the built-in voltage, but also has a large impact on the current close to the V_{bi} and above V_{bi} (see Supplemental Material [23]). Therefore, we introduce the band-bending parameter b according to

$$b = \frac{kT}{q}\left[\ln\left(\frac{q^2 N_v L^2}{2kT\varepsilon}\right) - 2\right], \quad (13)$$

based on a model by Simmons [18] (see Supplemental Material [23]). At V_{bi}, the current undergoes a transition from an exponential to a linear dependence on voltage. Because of the thickness dependence of the band-bending parameter, the linear current above V_{bi} depends inversely on L^3, while the exponential part below V_{bi} scales inversely with L. For voltages larger than the built-in voltage, the electric field becomes positive and the drift current starts to dominate. This is the well-known space-charge-limited current, described by Eq. (1). With the derived diffusion current, Eq. (12), we can now obtain the complete current through the device by summing the contributions of drift and diffusion, as shown in Fig. 2. The drift current starts exactly at the built-in voltage, well defined by φ_b-b. The analytical expression for the diffusion current now allows disentanglement of the drift and diffusion contributions to the current.

When comparing the expression for the diffusion-limited current for MIM diodes, Eq. (12), to the classical Shockley diode equation, Eq. (2), it is clear that there are subtle differences in the voltage dependence of the current density, as shown in the inset of Fig. 2. In order to match the slope of Eq. (12) using an effective barrier φ_b-b of 0.3 V, the ideality factor in Eq. (2) has to be adjusted to 1.2. This explains why experimentally in organic semiconductors without deep traps small deviations from unity of the ideality factor of about 0.2 were found when the Shockley equation was used for the analysis. This slight deviation from unity is therefore a fundamental property of organic MIM diodes, related to the charge transport. We note that the exact value of the deviation depends on the value of the effective applied voltage, φ_b-b-V. For most organic MIM diodes, the ideality factor is determined within 0.3 V below the built-in voltage (φ_b-b) [4], leading to an apparent ideality factor of ~1.2. For large barriers, carriers of the opposite sign will be injected, leading to trap-assisted recombination that will enhance the ideality factor [24].

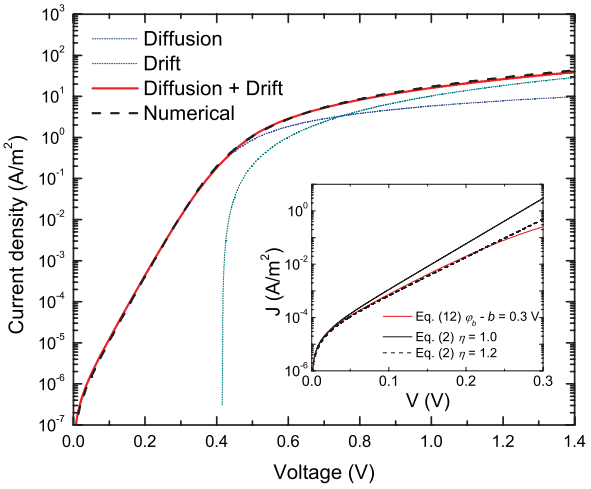

FIG. 2 (color online). Current density-voltage characteristics for a device with $\varphi_b = 0.7$ V, $\mu_p = 1 \times 10^{-9}$ m^2/Vs, $N_v = 3 \times 10^{26}$ m^{-3}, $L = 100$ nm, $T = 295$ K, and $\varepsilon = 3\varepsilon_0$. The dotted and solid lines are the analytically calculated characteristics for diffusion, drift, and the sum of drift and diffusion. The dashed line represents a numerical simulation [11] with exactly the same parameters. The inset shows a comparison between the calculated current for a MIM diode, Eq. (12), with φ_b-$b = 0.3$ V (lower curve) and the current calculated with the classical Shockley equation using an ideality factor of unity (upper curve). A good approximation is obtained using an ideality factor of 1.2 (dashed line).

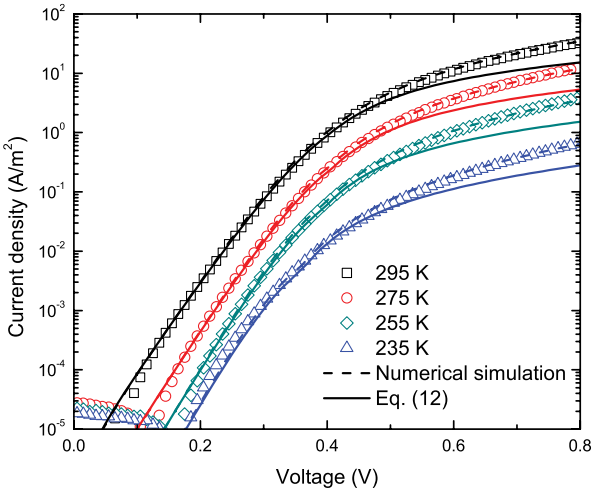

FIG. 3 (color online). Current-voltage characteristics of a PEDOT:PSS/PFO(80 nm)/MoO_3 hole-only MIM diode. PEDOT:PSS is grounded. The solid lines are fits to the experimental data (symbols) using the analytical equation for the diffusion-limited current. The deviation at higher voltages is due to the current being dominated by the drift term [SCLC, Eq. (1)] above the built-in voltage. The dashed lines represent numerical device calculations using a drift-diffusion solver [13] with exactly the same parameters as extracted from the analytical description.

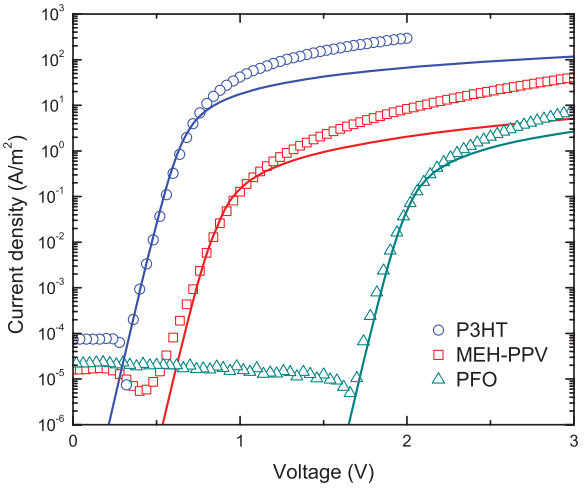

FIG. 4 (color online). Experimental current-voltage characteristics (symbols) of organic MIM diodes with an Ohmic MoO_3 contact and a ZnO collecting contact. The P3HT, MEH-PPV, and PFO layer thicknesses are 125, 120, and 180 nm. The solid lines are fits with Eq. (12).

To evaluate the applicability of the expression derived for the diffusion-limited current in MIM diodes we investigated a PFO hole-only diode with poly(3,4-ethylenedioxythiophene):poly(styrenesulfonic acid) (PEDOT:PSS) and MoO_3 contacts. MoO_3 provides an Ohmic contact even to PFO with a HOMO as deep as 5.8 eV [25]. The work function of PEDOT:PSS is around 5.2 eV. Hence, PEDOT:PSS serves as the collecting contact with an estimated energy barrier of about 0.6 eV. The exact value is not *a priori* known and may depend on the presence of interface dipoles and on Fermi level pinning due to interface trap states.

The experimental temperature-dependent current-voltage characteristics are shown in Fig. 3. At low bias the current increases exponentially with bias as expected for a diffusion-limited current. Above about 0.4–0.5 V the current becomes drift dominated and limited by the uncompensated charges of the injected holes, leading to a space-charge-limited current.

The parameters describing the charge-carrier mobility of PFO as a function of carrier density and temperature are well known [25]. The diffusion-limited current can now be fitted to the experimental data by adjusting the barrier in Eq. (12). The solid lines are a fit to the experimental data. A good agreement in the diffusion regime at $V < V_{bi}$ is obtained using a barrier φ_b of 0.67 V, with a band-bending parameter of 0.26 V [Eq. (13)]. The value for the barrier corresponds to previous estimates of the energy barrier between PFO and PEDOT:PSS of about 0.6 eV [25].

The dashed lines in Fig. 3 represent numerical device calculations using a drift-diffusion solver [13], with exactly the same parameters as used in the analytical fits. The numerical simulation contains both drift and diffusion, and band bending at the injecting contact is taken implicitly into account. The good agreement verifies the analytical expression of the diffusion-limited current in an organic MIM diode. The deviations for $V > V_{bi}$ are due to the current being dominated by the drift term at those voltages.

With the b parameter known, the analytical description for the diffusion-limited current in MIM diodes can be used to accurately determine the built-in voltage and injection barrier of the collecting contact. As an example, we investigated hole-only diodes of the polymers poly[3-hexylthiophene] (P3HT), poly[2-methoxy-5-(2-ethylhexyloxy)-1,4-phenylenevinylene] (MEH-PPV), and PFO with oxidic electrodes. MoO_3 was used as an Ohmic hole-injecting contact. ZnO is used as collecting contact. The work function of ZnO is about 4.0 eV. Taken into account the reported HOMO energies of -4.8, -5.1, and -5.8 eV this then yields expected energy barriers of 0.8, 1.1, and 1.8 eV for P3HT, MEH-PPV, and PFO, respectively.

The current-voltage characteristics are presented in Fig. 4. At very low bias, the current is below the detection limit of the measurement setup. With increasing bias, the exponential diffusion current exceeds the noise level. The solid lines represent fits of the diffusion-limited current in MIM diodes to the experimental data. The values for the barriers extracted are 0.93, 1.15, and 2.35 V. The obtained barriers agree well with the estimated energy barriers. This observation confirms the previous findings that the electron chemical potential is the main driving force for energy-level alignment at contacts

consisting of an organic semiconductor and transition-metal oxides [10].

In conclusion, we have demonstrated an analytical approach to model the diffusion current in organic metal-insulator-metal diodes with one Ohmic and one non-Ohmic contact. The analytical model accurately describes the voltage, temperature, and thickness dependence of the diffusion current and thus allows disentanglement of the drift and diffusion contributions to the current. This can substantially improve the accuracy of charge-transport measurements in organic-semiconductor diodes. The slight deviation of the apparent ideality factor from unity is characteristic of organic MIM diodes. Applying the analytic equation to experimental data provides an easy and accurate way of determining the built-in voltage and injection barrier in organic MIM diodes. Knowledge of the injection barrier from the diffusion current in forward bias is then an important ingredient for modeling of the injection-limited current in reverse bias, which is a subject of future study.

This work forms part of the research program of the Dutch Polymer Institute (DPI Project No. 660 and No. 678).

[1] N. F. Mott and R. W. Gurney, *Electronic Processes in Ionic Crystals* (Dover, New York, 1964).
[2] P. W. M. Blom, M. J. M. de Jong, and J. J. M. Vleggaar, Appl. Phys. Lett. **68**, 3308 (1996).
[3] W. Shockley, Bell Syst. Tech. J. **28**, 435 (1949).
[4] G. A. H. Wetzelaer, L. J. A. Koster, and P. W. M. Blom, Phys. Rev. Lett. **107**, 066605 (2011).
[5] W. Schottky, Naturwissenschaften **26**, 843 (1938).
[6] H. J. Bolink, E. Coronado, D. Repetto, and M. Sessolo, Appl. Phys. Lett. **91**, 223501 (2007).
[7] K. Morii, M. Ishida, T. Takashima, T. Shimoda, Q. Wang, M. K. Nazeeruddin, and M. Graetzel, Appl. Phys. Lett. **89**, 183510 (2006).
[8] D. Kabra, L. P. Lu, M. H. Song, H. J. Snaith, and R. H. Friend, Adv. Mater. **22**, 3194 (2010).
[9] P. de Bruyn, D. J. D. Moet, and P. W. M. Blom, Org. Electron. **13**, 1023 (2012).
[10] M. T. Greiner, M. G. Helander, W.-M. Tang, Z.-B. Wang, J. Qiu, and Z.-H. Lu, Nat. Mater. **11**, 76 (2012).
[11] J. G. Simmons, Phys. Rev. Lett. **15**, 967 (1965).
[12] S. M. Sze, *Physics of Semiconductor Devices* (Wiley-Interscience, New York, 1981).
[13] L. J. A. Koster, E. C. P. Smits, V. D. Mihailetchi, and P. W. M. Blom, Phys. Rev. B **72**, 085205 (2005).
[14] P. H. Nguyen, S. Scheinert, S. Berleb, W. Brütting, and G. Paasch, Org. Electron. **2**, 105 (2001).
[15] M. C. J. M. Vissenberg and M. Matters, Phys. Rev. B **57**, 12964 (1998).
[16] W. F. Pasveer, J. Cottaar, C. Tanase, R. Coehoorn, P. A. Bobbert, P. W. M. Blom, D. M. de Leeuw and M. A. J. Michels, Phys. Rev. Lett. **94**, 206601 (2005).
[17] N. I. Craciun, J. J. Brondijk, and P. W. M. Blom, Phys. Rev. B **77**, 035206 (2008).
[18] J. G. Simmons, J. Phys. Chem. Solids **32**, 1987 (1971).
[19] V. D. Mihailetchi, P. W. M. Blom, J. C. Hummelen, and M. T. Rispens, J. Appl. Phys. **94**, 6849 (2003).
[20] J. Hwang, E. G. Kim, J. Liu, J.-L. Bredas, A. Duggal, and A. Kahn, J. Phys. Chem. C **111**, 1378 (2007).
[21] J. C. Blakesley and N. C. Greenham, J. Appl. Phys. **106**, 034507 (2009).
[22] I. Lange, J. C. Blakesley, J. Frisch, A. Vollmer, N. Koch, and D. Neher, Phys. Rev. Lett. **106**, 216402 (2011).
[23] See Supplemental Material at http://link.aps.org/supplemental/10.1103/PhysRevLett.111.186801 for details regarding band bending and additional comparison with numerical simulations.
[24] G. A. H. Wetzelaer, M. Kuik, H. T. Nicolai, and P. W. M. Blom, Phys. Rev. B **83**, 165204 (2011).
[25] H. T. Nicolai, G. A. H. Wetzelaer, M. Kuik, A. J. Kronemeijer, B. de Boer, and P. W. M. Blom, Appl. Phys. Lett. **96**, 172107 (2010).